



Post-Buckling Shear Behavior of Corrugated Steel Web girders

*Prof. Dr. S. A. Hassanein, Assoc. Prof. Dr. E. S. Salem,
Eng. A. M. Mohmoud*

Civil Engineering Department, Faculty of Engineering Al-Azhar University

ملخص البحث

يُقدّم هذا البحث اختبارات معملية، ونمذجة عددية؛ لدراسة سلوك القص اللاحق للانبعاج في الكمرات المعدنية ذات العصب المُموج، حيث تمّ تصنيع واختبار كمرتين ذات مقياس مناسب؛ إحداهما ذات عصب مُموج على شكل شبه منحرف، والأخرى ذات عصب مُموج على شكل منحنى دالة (sine)، وقد تمّ تحميل الكمرتين حتى الانهيار، وقياس الانفعال والترخيم في الأماكن المحددة، كما تمّت ملاحظة وتسجيل حدوث الانبعاج الموضعي والكلبي للعصب المُموج، وتبيّن قدرة العصب على مقاومة قوّة قص إضافية بعد حدوث عملية الانبعاج، وذلك نتيجة تولد قوّة شد في منطقة العصب المنبجج، تلك القوّة التي تتركز كلاً عند الشفتين العلوية والسفلية للكمر، مما ينتج عنه تأثير ملحوظ لجساءة هاتين الشفتين على هذه القوّة الوليدة، وبالتالي سلوك هذه الكمرات في مرحلة ما بعد الانبعاج، علاوة على ذلك تمّت مقارنة النتائج التي تمّ استنباطها باستخدام النمذجة العددية بالنتائج المعملية والتي جاءت متوافقة ومؤكدة لها.

Abstract

This paper presents an experimental and a Finite element analysis for post-buckling behavior of corrugated web steel girders. Two girders with corrugated steel webs are fabricated and tested. The first one has a trapezoidal corrugated web while the other one has a sinusoidal corrugated web. All specimens are loaded in four-point loading test. Both local and global buckling are observed. Tension field action was developed after web buckling had been occurred. Plastic hinges are formed in flanges at the regions where web buckling and tension field have developed. The flexural stiffness of the flanges contributes significantly to the shear strength resisted by tension field action. Furthermore, Finite element analyses were conducted to study the behavior of the tested girders. Nonlinear materials analysis and initial imperfection were included. Good agreement can be observed between the experimental and finite element analysis. Ultimate load, maximum deflection, and failure mechanism were discussed.

Keywords: *corrugated web, post-buckling shear behavior, tension field action, finite element analysis.*

1. Introduction

Corrugated steel webs are used in both I-girder and box girder to enhance the shear resistance of these girders and reduce their weights, compared to flat web girders. Easley and Mcfarland in 1969 [1] started that researches. Experimental and theoretical researches on shear strength of trapezoidal corrugated steel web girders have been conducted by Easley and Mcfarland [1], Linder and Aschinger [2], Elgaaly et al [3], Sause and Braxtan [4]. Based on their studies, local and global elastic shear buckling strengths have been deduced. Many formulas have been introduced to calculate the interactive shear strength of corrugated web girders. Abbas [3] proposed a verified equation that showed a good agreement with available experimental test results. Until 1960, design of plate girders was based on buckling, however, acknowledging the fact that the girders can carry loads after buckling led to the development of new theories. Wagner [5] and Kuhn [6] developed the concept of diagonal tension theory of flat web girders subjected to shear loading. Basler and Thurlimann [7] developed the limited

tension field theory for the post-buckling of flat web girder in shear. The British standard adopted the Cardiff model [8], which considers a diagonal tension band with failure occurring when the yield spreads all over the band and hinges form in the flanges. Euro code3 EN1993-1-5 [9] adopted Hoglund's model [10] which is an extension of an earlier theory that is based on the rotated stress field method. Post-buckling strength is achieved when the web' diagonal develops a tension field. Prior to that, the shear stress distribution is uniform all over the web panel [11]. Leblouba et al. [12] observed that the tension-field action, in corrugated steel web girders, is affected by the contribution of the flexural stiffness of the flanges.

2. Experimental study

2.1. Fabrication of test specimens

Two corrugated steel web girder specimens were fabricated [13]. One of the specimens has a trapezoidal profile (IGW1), while the other one has a sinusoidal profile (IGW2). The geometry of specimens IGW1 and IGW2 is shown in Figs. 1 and 2, respectively. At supports and loading points, stiffeners are provided.

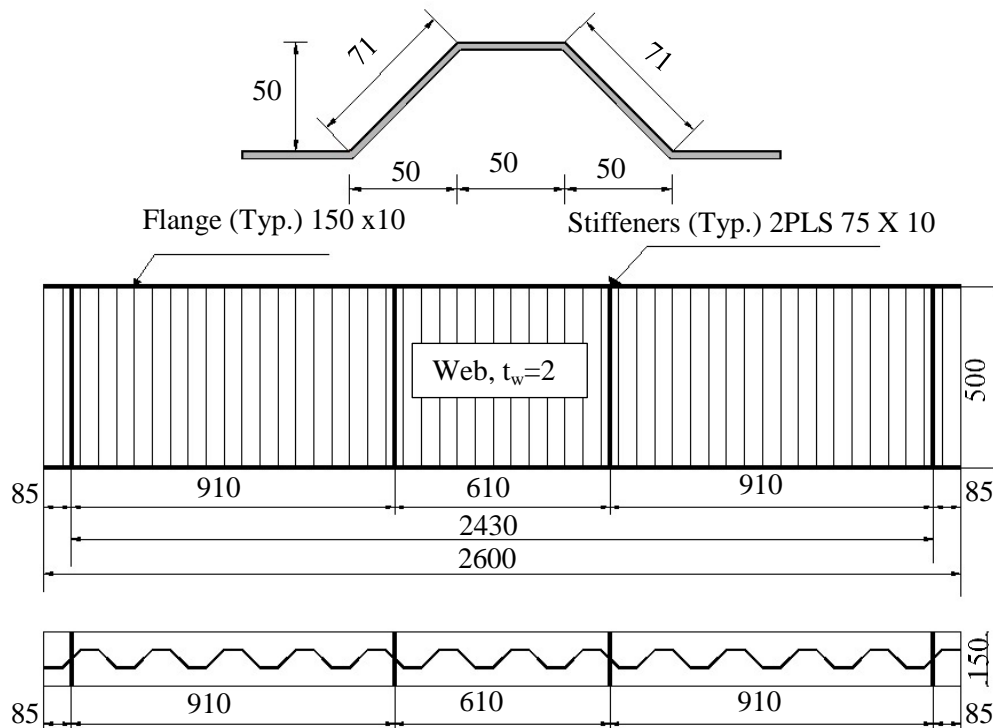


Fig. 1. Specimen (IGW1) (all dimensions are in mm)

The specimens were designed to be loaded in four points bending with two loads and two reactions to produce constant moment region. The nominal specimen dimensions are summarized in Table 1. Nominal and measured plate thicknesses of the two specimens are summarized in Table 2. The fabrication process is shown in Fig. 3.

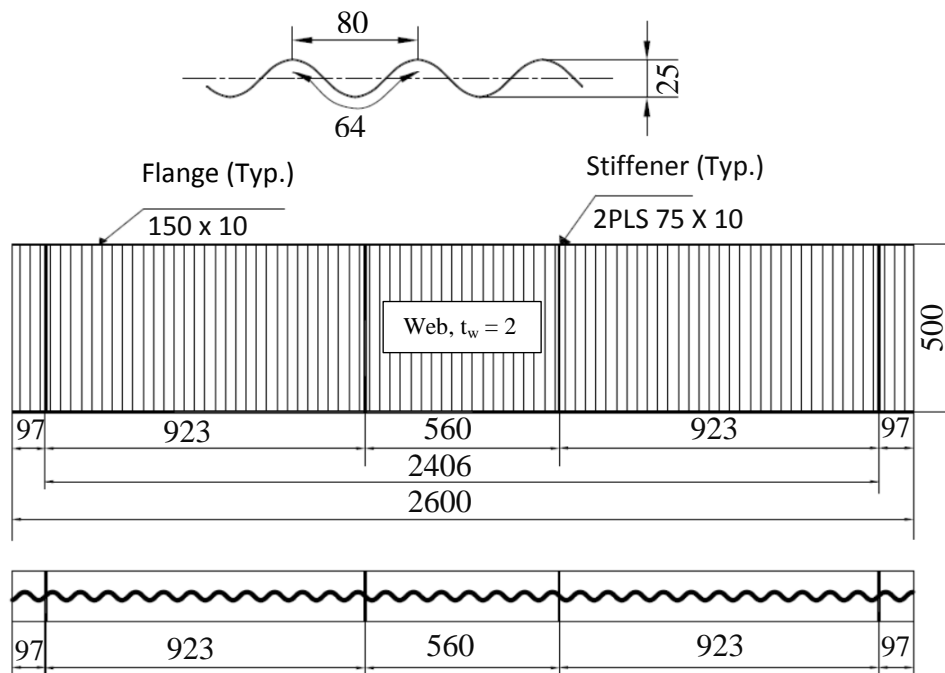


Fig. 2. Specimen (IGW2) (all dimensions are in mm)

Table 1. Nominal specimen dimensions

Specimen No.	Effective span (mm)	Profile type	h_w / t_w	Section		
				Top flange (mm)	Web thick (mm)	Bottom flange (mm)
IGW1	2406	trapezoidal	250	150 x 10	2	150 x 10
IGW2	2430	sinusoidal	250	150 x 10	2	150 x 10

Table 2. Nominal and measured specimen thicknesses

Specimen No	Component	Nominal thickness (mm)	Measured thickness (mm)
IGW1	flanges	10	10.45
	web	2	2.01
	stiffeners	10	10.5
IGW2	flanges	10	10.4
	web	2	2.21
	stiffeners	10	10.49

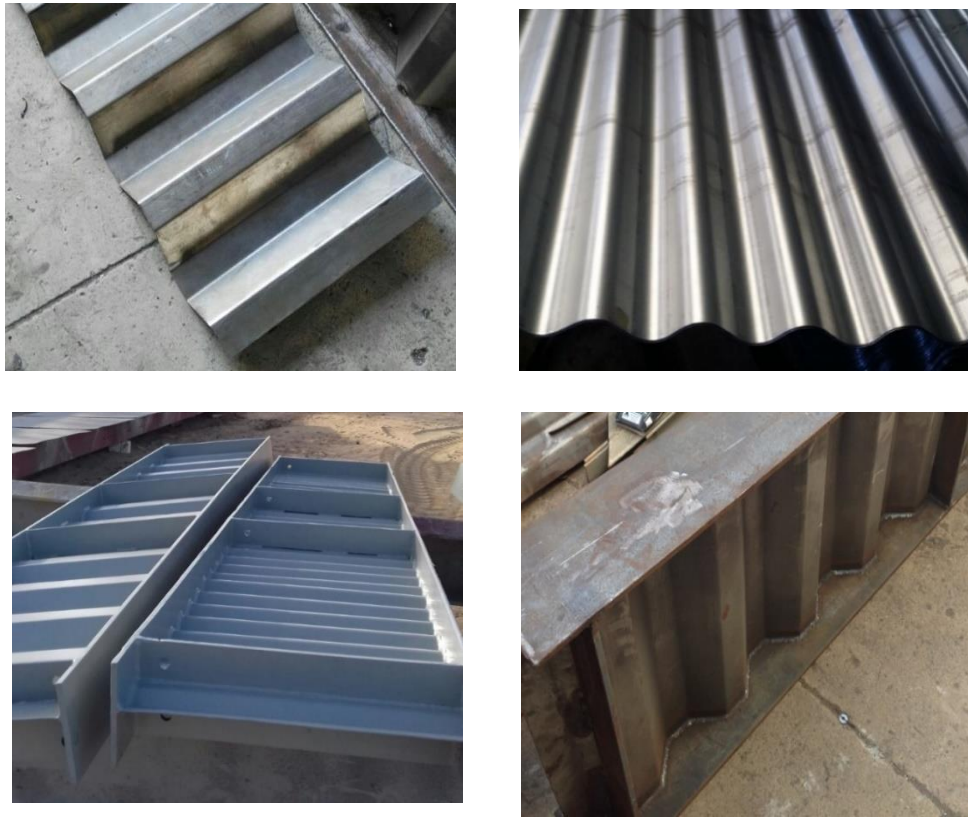


Fig. 3. Fabrication of specimens

2. Material properties

Six standard tensile coupon specimens (three from the flanges and three from the web as shown in Fig. 4) were cut from the steel specimen plates, prior to fabrication, to determine their mechanical properties. Tables 3 shows the obtained average mechanical properties (yield and ultimate strengths and elongation percentage).



Fig. 4. Tensile coupon specimens

Table 3. Average mechanical properties of steel plates

Specimen No.	Coupon Type	Yield stress (MPa)	Ultimate strength (MPa)	Elongation %
IGW1	Flange	418	530	25
	Web	405	528	15
IGW2	Flange	418	530	25
	Web	560	625	8

2.3 Testing

2.3.1 Instrumentation

Fig. 5 shows the typical instrumentations for test specimens IGW1 and IGW2. The test specimens were instrumented with a combination of displacement transducers (LVDT) and uniaxial strain gauges. The instrumentation scheme was designed to measure the web shear strains and flange bending strains. A total of 10 uniaxial strain gauges and 2 LVDTs were used. The test data was acquired and processed using data acquisition system and personal computer. Three strain gauges were installed on both bottom and top flanges. The remaining strain gauges were located near the support on the corrugated web to measure the shear strain. To use a uniaxial strain gauge to measure the shear strain, it was oriented 45° to the vertical axis. One LVDT was vertically located at the bottom flange at mid-span to measure the vertical displacement and the other LVDTs was horizontally located at the edge of the top flange at mid-span to measure the transverse displacement. These locations are shown in Fig. 5.

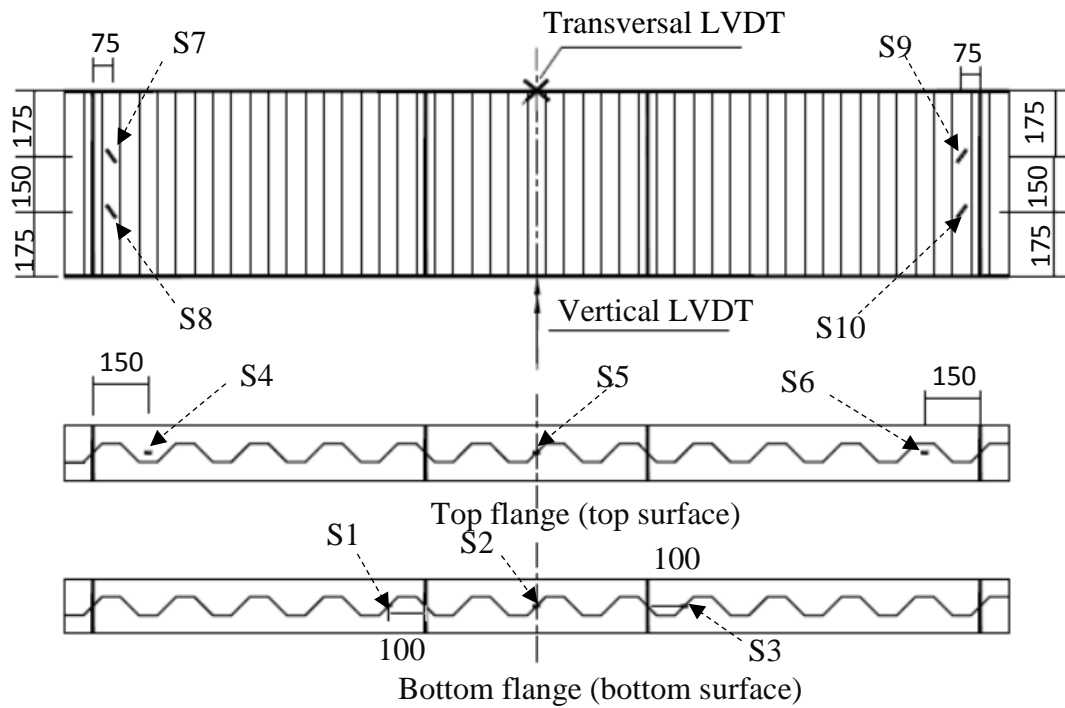


Fig. 5. Instrumentations of specimens (all dimensions are in mm)

2.3.2 Test set-up

The tests were performed using a Five-Million-Newton Universal testing machine in National Research Center Laboratory, Cairo, Egypt. The main characteristics of the test setup and fixtures are shown in Fig. 6. The specimen is mounted on a stiffened steel pedestal.

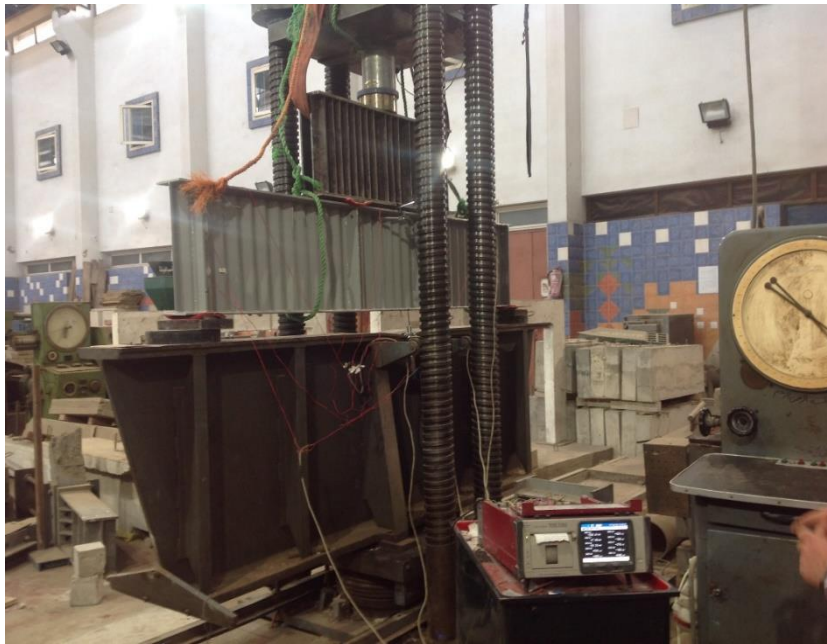


Fig. 6. Test set-up

Industrial slings were provided at the ends of the test setup to restrain the sudden movement of the specimen at failure. The strain gauges were initialized after ensuring that all instruments were working properly.

2.4 Experimental results and discussion

2.4.1 Specimen IGW1

The load-deflection curve at mid-span for specimen IGW1 is shown in Fig. 7. As anticipated, the girder failed suddenly by web buckling. In a dynamic manner, the load dropped from 530 kN to 115 kN due to buckling of web. The web buckling occurred in the three folds closed to left support. The buckled waves extended over both the inclined and longitudinal folds as shown in Fig. 8.

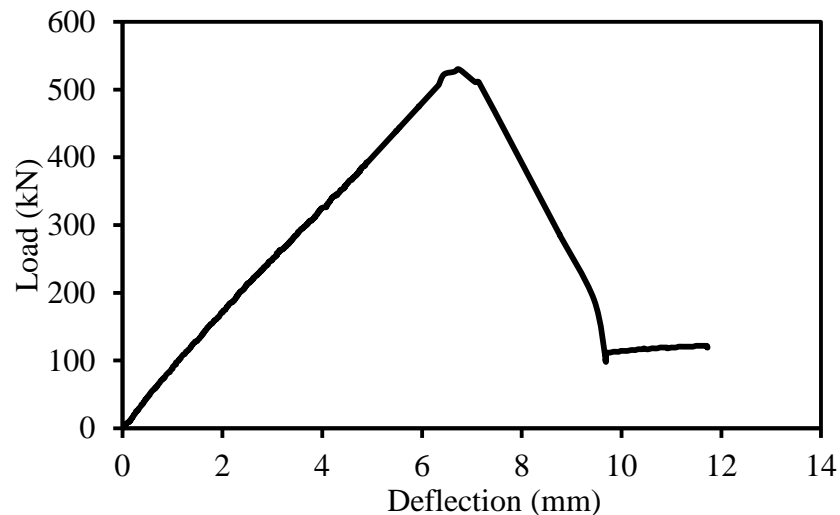


Fig. 7. Load–deflection curve at mid-span, IGW1

Plastic hinges were formed in both top and bottom flanges at the location of web buckling. The load-deflection curve can be divided into two main parts. The first part is limited by the load peak and is characterized by being close to a linear load-deflection relationship. The second part is the post-peak load stage. For design purposes, the ultimate nominal strength should be taken as the end of linear part (peak load). Although the post-buckling, with its substantially low load level (in this specimen), is not important for the design purpose, a study of this stage is important to discuss the problem of suddenly failure and to enhance the ductility behavior for steel girder with corrugated web. Once the web was buckled, a tension field action was developed in buckled panel. The tension field forces anchor in the top and bottom steel flanges, with the formation of plastic hinges in the flanges. Four plastic hinges were formed in top and bottom flanges. So, the flexural stiffness of the flanges significantly affects the post-buckling shear behavior of steel girder with corrugated web. The experimental web shear strains and flange normal strains versus the applied load at different locations are shown in Fig. 9.

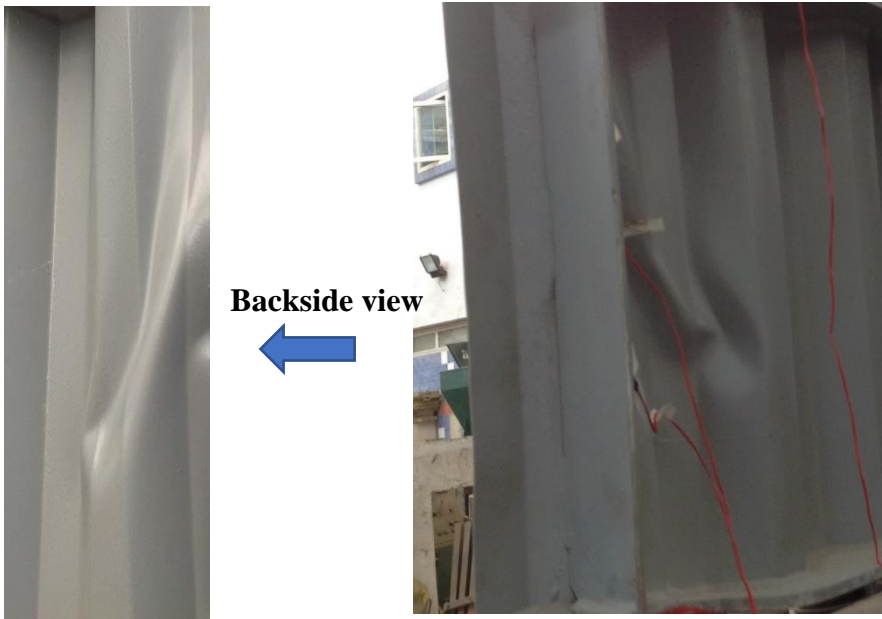


Fig. 8. Web buckling shape after failure specimen IGW1

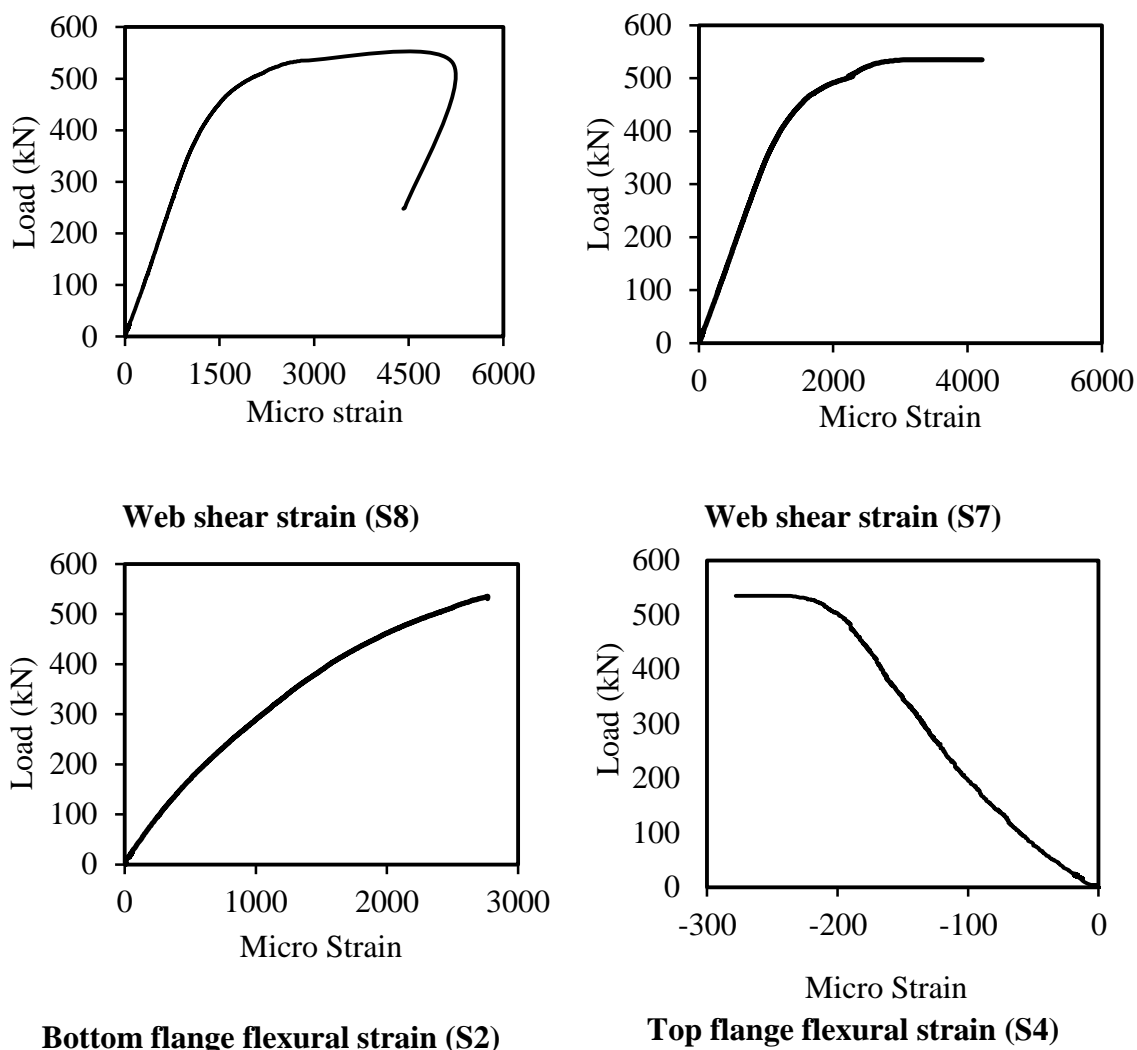


Fig. 9. Shear and flexural strains versus applied load for specimen IGW1

2.4.1 Specimen IGW2

Unlike specimen IGW1, specimen IGW2 was able to undergo large deflection after the onset of yielding and prior to fracture (Fig. 10). Plastic hinges were formed in top and bottom flanges at the anchorage location of the tension field which was developed after web buckling. The good ductile behavior that shown by specimen IGW2, unlike specimen IGW1, may be due to the dense sinusoidal corrugation which increases the post buckling resistance of the web. As the deflection increased, a fracture line was developed in the web. The fracture growth from top to bottom and was inclined with 45°, approximately, and perpendicular to the tensile stress direction as shown in Fig. 11.

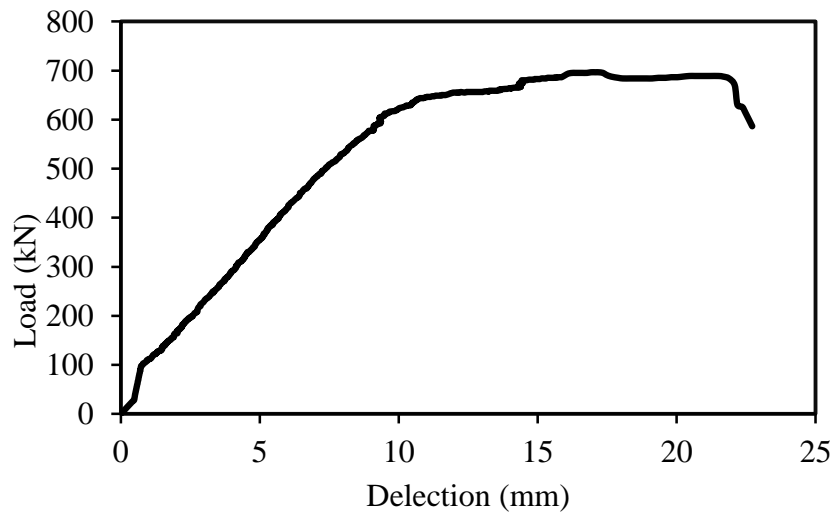


Fig. 10. Load–deflection curve at mid-span, IGW2

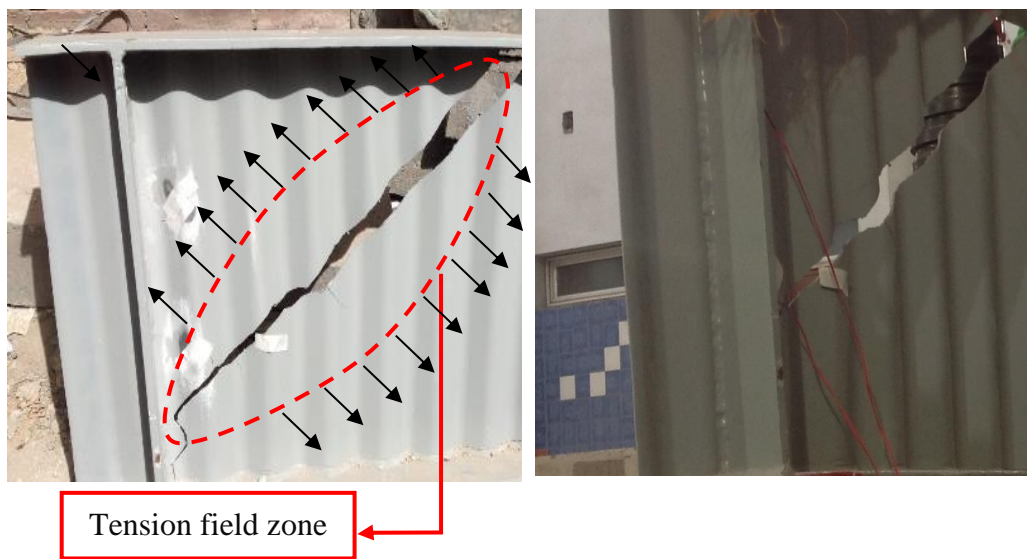


Fig. 11. Web fracture, IGW2

The experimental web shear strains and flange normal strains versus the applied load at different locations are shown in Fig. 12. The large values for flexural strains in top and bottom flanges reflect the ductile behavior of specimen IGW2 at failure.

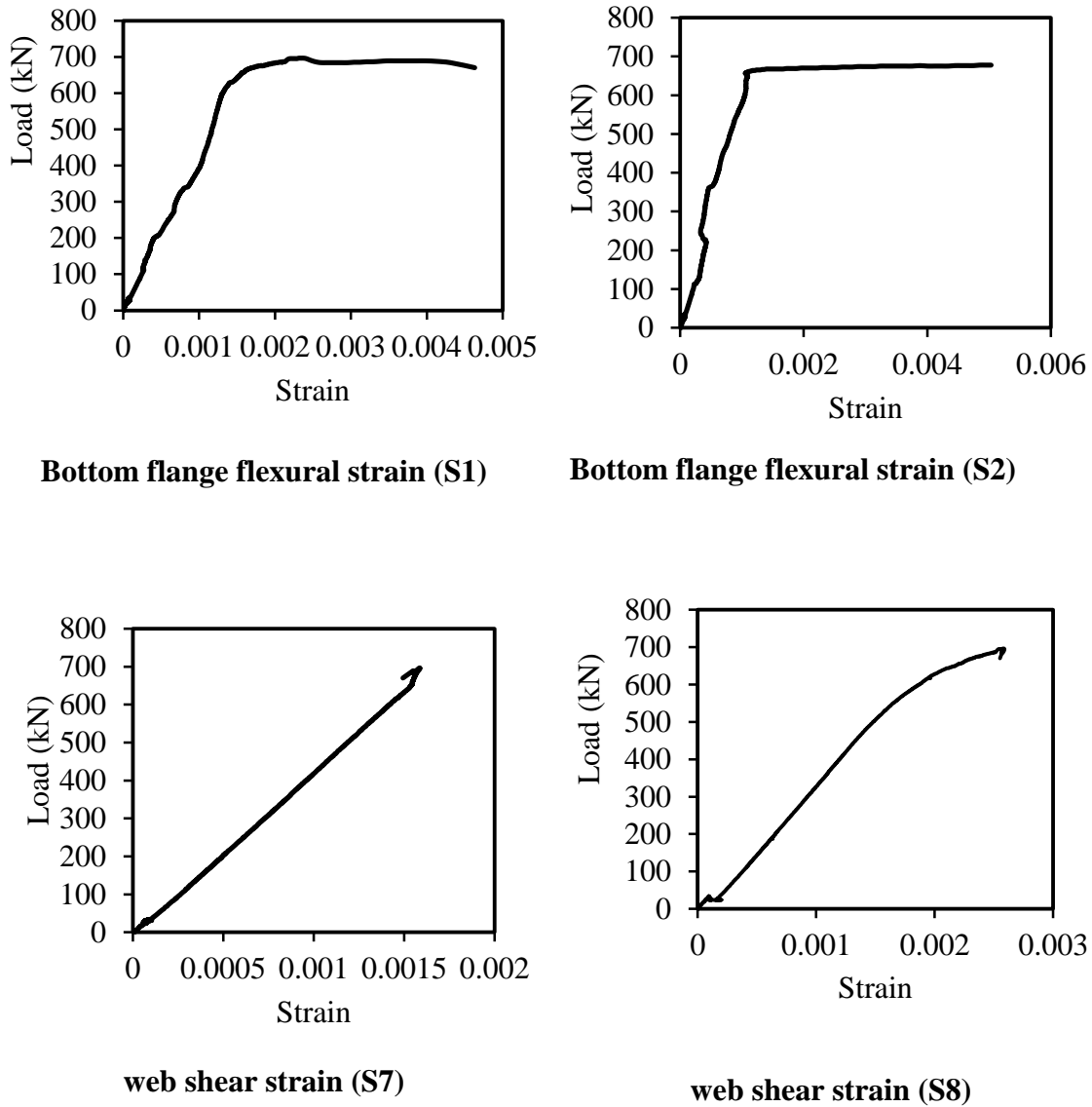


Fig. 12. Shear and flexural strains versus applied load for specimen IGW2

3. Finite Element Modeling

A three-dimensional nonlinear finite element modeling procedure was used to accurately assess the behavior and capacity of corrugated web steel girders. The commercial general-purpose FE package ABAQUS V6.14 is used in this study [14]. ABAQUS 6.14 provides complete material and geometric modeling capabilities with a variety of available element types. A four-node doubly curved shell element with reduced integration (S4R) is used to model the flanges and corrugated web. This

element is suitable for complicated buckling behavior. The S4R element has 6 degrees of freedom per node and provides an accurate solution to most applications. In addition, S4R element accounts for finite strain and is suitable for large strain analysis, including inelastic deformation of material [14].

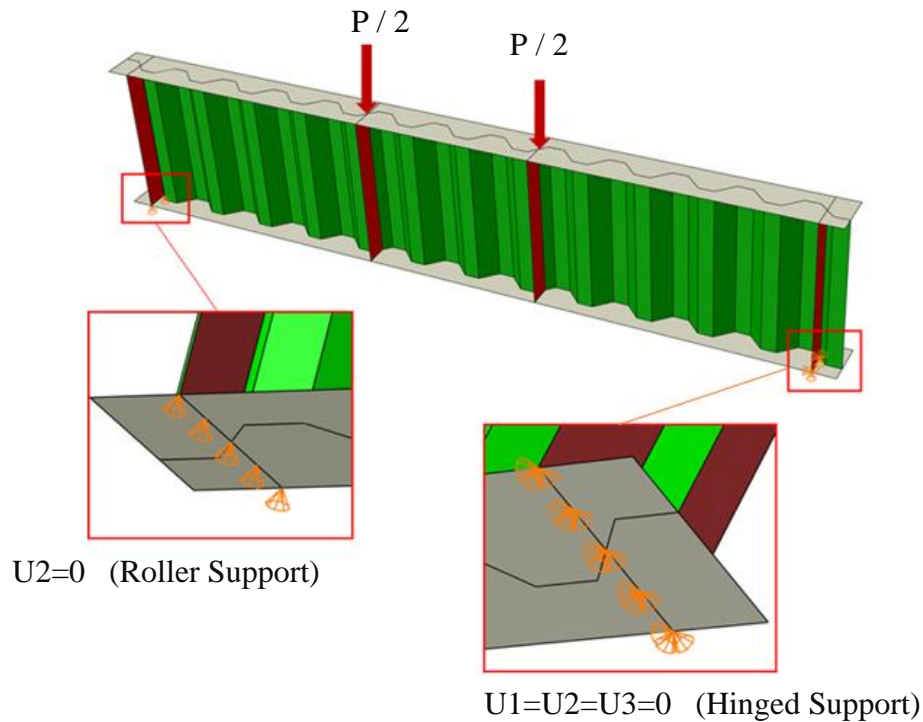


Fig. 13. Loading and boundary condition for typical finite element model

Since local and global buckling of corrugated web are very sensitive to large strains, the S4R was used in this study to ensure the accuracy of the results. Loading and boundary conditions for typical finite element model are shown in Fig. 13.

3.1 Results and discussions

The developed finite element models for steel girders with corrugated web were verified using the experimental results. The load-mid span deflection and failure modes that were obtained from experimental tests were compared with finite element results. As shown in Figs. 14 and 15, the Finite element results agree well with experimental results.

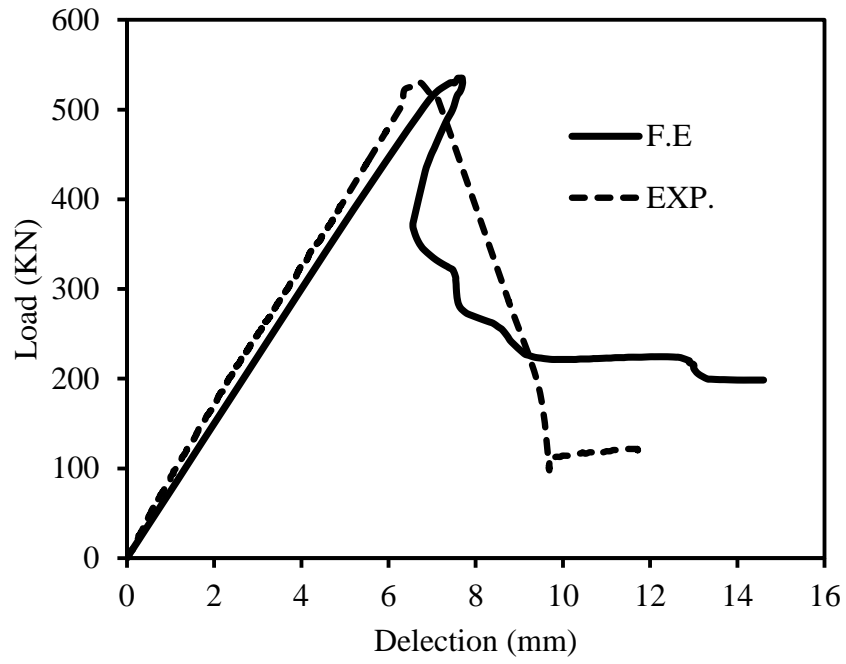


Fig. 14. Load-mid span deflection curve, IGW1.

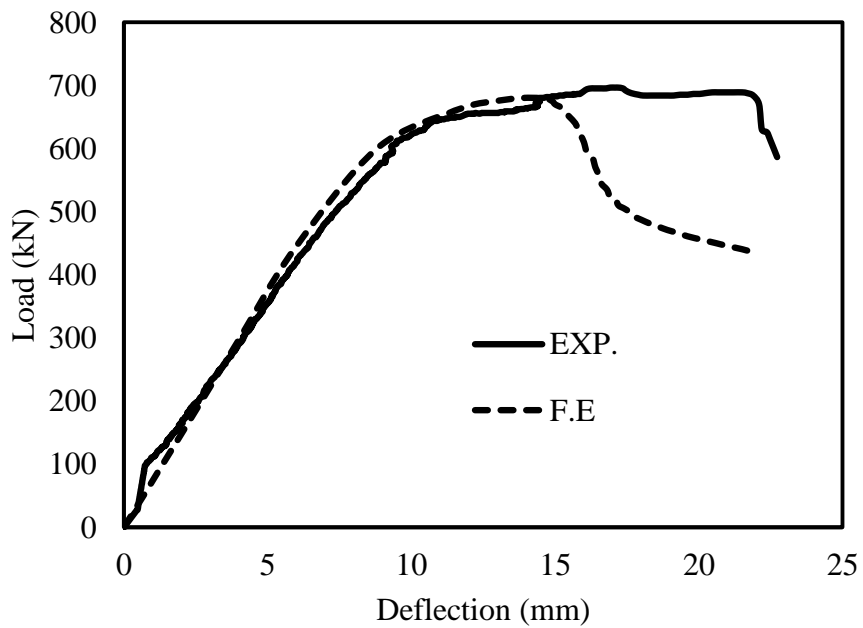


Fig. 15. Load-mid span deflection curve, IGW2.

The failure mode experimentally observed is confirmed by finite element modeling. With buckling propagation, a tension field zone was development in the web and plastic hinges were formed in top and bottom flanges as shown in Figs. 16 and 17. The results

obtained from finite element models have shown that the plastic deformations have been concentrated at the plastic hinge locations in the top and bottom flanges, at the locations of anchoring the tension field developed in the corrugated web.

To confirm the plastic hinge locations, the plastic strain contours in the axial direction (direction 1-1) were plotted as shown in Figs. 16 and 17 for specimens IGW1 and IGW2, respectively. It can be seen that the plastic strains were concentrated at four regions, two in the top flange and two in the bottom flange. These regions represent the plastic hinge locations.

For specimen IGW1, the ultimate failure load from the experimental test was 530 kN at a deflection of 6.7mm, while the ultimate failure load predicted from the finite element analysis was 535 kN at a deflection of 7.7 mm. The finite element failure load was 1% larger than observed in the experimental test.

For specimen IGW2, the ultimate failure load from experimental test was 690 kN at a deflection of 22 mm. The ultimate failure load predicted from the finite element model was 680 kN at a deflection 15 mm. The experimental load failure was 2 % larger than that observed in finite element model..

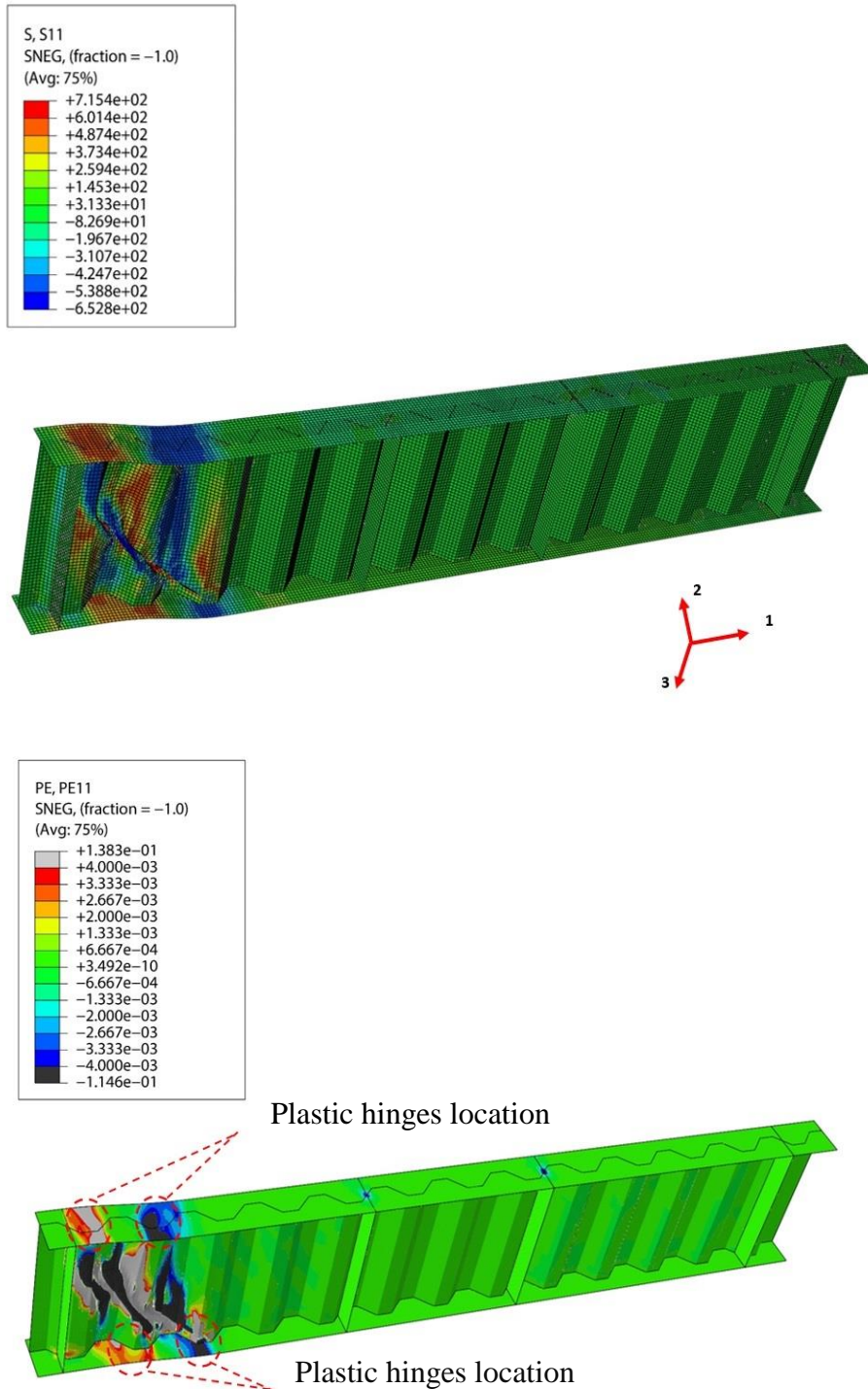


Fig. 16. Normal stresses and plastic strains for specimen

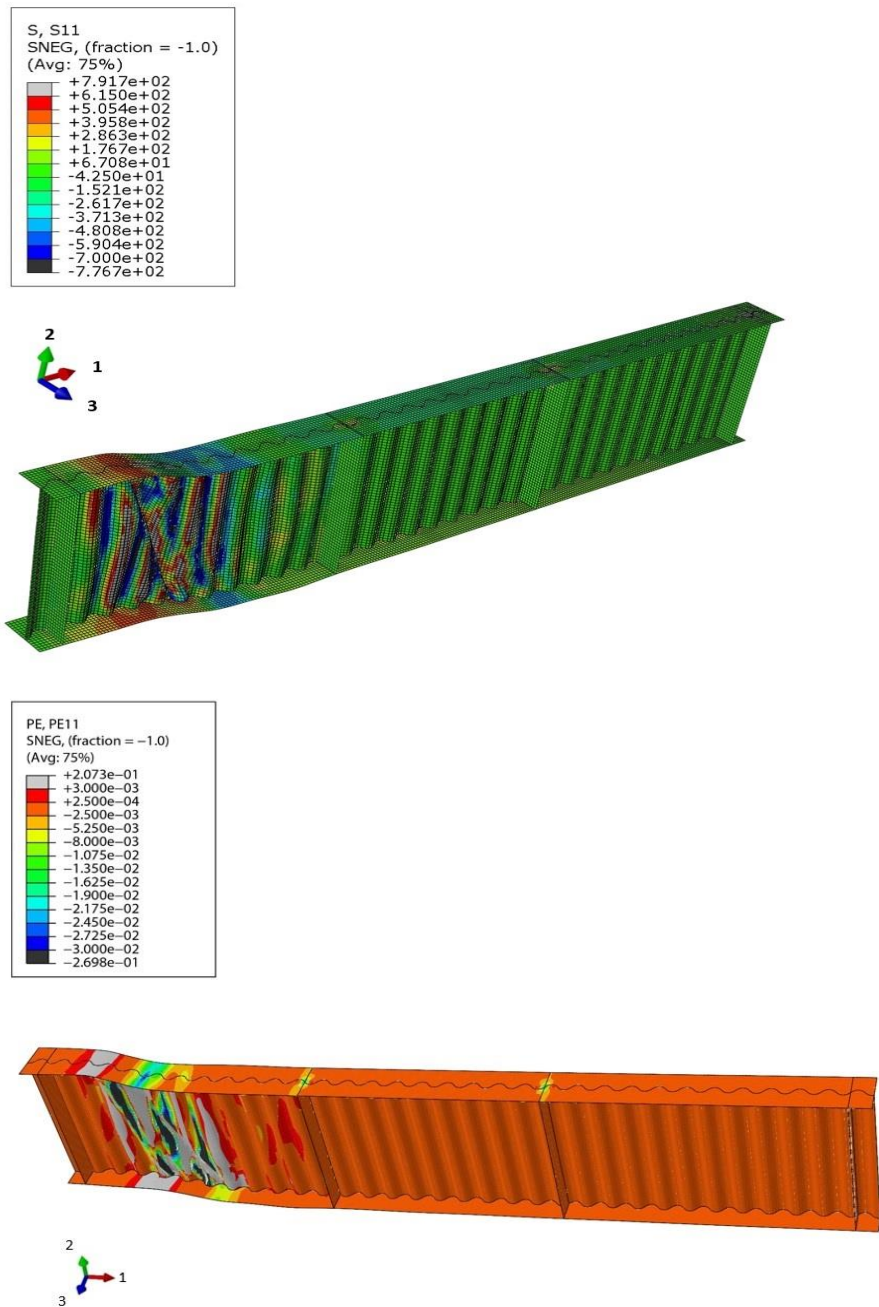


Fig. 17. Normal stresses and plastic strains for specimen

4. Conclusions

In this study, an experimental and finite element analysis of corrugate steel web girders were performed to investigate their post-buckling shear behavior. The following conclusions are drawn from this study:

1. An additional shear strength of corrugated steel web is developed after web buckling. The additional shear strength is provided by a tension field mechanism.
2. The flexural stiffness of flanges significantly affects the post-buckling behavior of steel girders with corrugated web.
3. The dense sinusoidal profile for corrugated web enhanced the post-buckling behavior, where a good ductile behavior was observed.
4. Tension field action, developed after web buckling, is significantly important to achieve a ductile behavior for steel girder with corrugated web.

References

1. Easley, J. T., & McFarland, D. E. (1969). Buckling of light-gage corrugated metal shear diaphragms. *Journal of the Structural Division*, 95(7), 1497-1516.
2. Lindner J, Aschinger R. Grenzscherbtragfähigkeit von I-trägern mit trapezförmig profilierten Stegen. *Stahlbau* 1988; 57(12):377–80.
3. Elgaaly, M., Hamilton, R. W., & Seshadri, A. (1996). Shear strength of beams with corrugated webs. *Journal of Structural Engineering*, 122(4), 390-398.
4. Sause, R., & Braxtan, T. N. (2011). Shear strength of trapezoidal corrugated steel webs. *Journal of Constructional Steel Research*, 67(2), 223-236.
5. Wagner, H. (1931). Flat sheet metal girders with very thin webs, Part I-General theories and assumptions. *National Advisory Committee for Aeronautics, Technical Memo*, (604).
6. Kuhn, P. (1956). *Stresses in aircraft and shell structures*. McGraw-Hill.
7. Basler, K., & Thurlimann, B. (1960). Carrying capacity of plate girders, final report. In *6th Congress of IABSE, Stockholm*.
8. Porter, D. M., Rockey, K. C., & Evans, H. R. (1987). *The collapse behaviour of plate girders loaded in shear*. University College Department of Civil and Structural Engineering.
9. EN 1993-1-5, Eurocode 3, Design of steel structures, Part 1-5. Plated structural Elements, 2006.
10. Hoglund, T. (1973). *Design of thin plate I girders in shear and bending with special reference to web buckling*. Department of Structural Mechanics and Engineering, Royal Institute of Technology.
11. Galambos, T. V. (Ed.). (1998). *Guide to stability design criteria for metal structures*. John Wiley & Sons.
12. Leblouba, M., Junaid, M. T., Barakat, S., Altoubat, S., & Maalej, M. (2017). Shear buckling and stress distribution in trapezoidal web corrugated steel beams. *Thin-Walled Structures*, 113, 13-26.
13. Mahmoud, A.M, Behavior of composite box girder with steel corrugated webs. Ph.D. thesis, Al-Azhar University, Faculty of Engineering, Civil Engineering Department 2018, under revision.
14. ABAQUS Standard User's Manual. The Abaqus Software is a product of Dassault Systems Simulia Corp., Providence, RI, USA Dassault Systems, Version 6.14, USA; 2014.